Journal of Harbin Engineering University
ISSN: 1006-7043
Vol 44 No. 11
November 2023

Finite Element Analysis of Non-Newtonian Fluid Flow for Viscoelastic Assessment

Ritesh Yadav[1] and Kamna Khetarpal[2]
[1,2]Department of Physics, Dr. A. P. J. Abdul Kalam University, Indore
Corresponding Author: ritesh.yadav09@gmail.com

Abstract: This article takes a look at the challenge of numerically approximating non-Newtonian fluid flow with a Unconfined surface. The movement of newly mixed concrete is specifically targeted by this solution. The behaviour of industrial mixes frequently resembles that of non-Newtonian fluids, which means that they display a yield stress that must be overcome before the cf. mixture can flow. The discretization of the problem through the use of the finite element method and the mathematical formulation of the problem are receiving the majority of the focus and attention. The numerical method that has been explained is implemented into the process of solving multiple issues.

Keywords: *Finite element; Viscoelastic, Unconfined surface; non-Newtonian fluid.*

1. INTRODUCTION

The investigation of the dynamics of fluids that do not fall within the category of Newtonian fluids presents a significant challenge, and the majority of their relevance lies in the realm of industrial purposes cf. (R.P. Chhabra, J.F. Richardson, 1999). Newton's rule of viscosity is simply unsuitable for the description of macromolecular liquids as well as a variety of mixes (for example, new concrete, mortar), in which the viscosity coefficient may radically alter with the change in the fluid's rate of strain. It is important to keep in mind that incompressible fluids are distinguished by two material constants, namely, their density and viscosity. The experimental description of the incompressible non-Newtonian fluid is far more sophisticated, as contrasted with the previous sentence (R.B. Bird, et. al., 1987). In this article, we discuss the Viscoelastic models of fluids that belong to the class of the so-called time independent fluids or the generalised Newtonian fluids. In these types of fluids, the local viscosity coefficient depends only on the most recent local values of the rate of strain and does not exhibit memory effects.

There are three equations that make up the mathematical explanation of this issue: the continuity equation, the Navier-Stokes system of momentum equations, and the constitutive equation. Even if the convective elements are removed, the generalisation of the Stokes issue will still be nonlinear since the constitutive equation is not linear and so is the generalisation of the Stokes problem.

The issue that will be looked at is the use of numerical simulations to analyse the flow of new concrete; for more information, see (B. Patzák, 2006). It is possible to think about concrete in its fresh condition as a fluid, given that a particular degree of flow can be obtained and that the concrete is homogenous (for an example, see) (C. Ferraris, 2001). Shear stress and shear rate are two notions that are used in the process of describing the flow of a fluid (D. Beaupre, S. Mindess, 1998).

It is often believed that concrete, when considered a fluid, has the characteristics of a Bingham fluid (cf). (R.B. Bird, et. al., 1987). In this particular instance, the properties that best describe the fluid are its yield stress and its plastic viscosity. The model's parameters may be determined using Viscoelastic techniques, and their values are dependent on the quality of the concrete's constituent materials (cf (P. Coussot, et. al., 1996). Obviously, the model is unable to explain the qualitative state of the concrete or the chemical changes that take place inside it, but it is able to offer a fair approximation for the fresh condition at least for a short amount of time.

In addition, an approximation has to be found for the issue with the Unconfined surface. The surface of the fluid is not known in advance, but figuring it out is part of the answer. Either the technique of interface capture or the method of interface tracking may be used to describe the ways that are extensively employed (cf (S.R. Ransau, 2002). In this particular piece of research, the level set approach is used. Regarding the use of the volume of fluid approach

within the context of the turbulent three-dimensional flow.

The discretization of the mathematical issue is accomplished with the help of the finite element technique. The strategy for stabilising is based on an adaptation of the Galerkin Least Squares method in accordance with the (T. Gelhard, et. al., 2005).

1. MODEL BASED ON MATHEMATICAL EQUATIONS

1.1. FLUID MODEL

A non-Newtonian fluid may be described mathematically using the incompressible Navier-Stokes system of equations and the Viscoelastic constitutive equation for the fluid. Both of these equations describe the fluid's rheology. In addition to this, it is essential to take into consideration the Unconfined surface area of the fluid. Let us refer to the region that the fluid is occupying as Ω_t⊂R^2. The boundary $\partial\Omega$_t consist of numerous fraction.

$$\partial\Omega_t = \Gamma_D \cup \Gamma O \cup \mathcal{I}_t,$$

Where the boundary $\mathcal{I}_t$ is the Unconfined surface component of the boundary (the interface between the fluid of our interest and the fluid/gas that is around it), and where the boundary I t is the section of the boundary that we are interested in.

The issue that is being addressed may be described using the following set of equations, which are derived from the conservation laws:

$$\frac{\partial \rho}{\partial t} + \nabla \cdot (\rho \mathbf{v}) = 0 \qquad (1)$$

In the event that we are dealing with an incompressible fluid (that is, $\rho \equiv$ constant), Equation (1) may be rewritten as

$$\nabla \cdot \mathbf{v} = 0 \qquad (2)$$

In addition, the equations for momentum, which are part of the Navier-Stokes system of equations, are presented in the form.

$$\frac{\partial(\rho v_i)}{\partial t} + \sum_j \frac{\partial(\rho v_i v_j)}{\partial x_j} = \sum_j \frac{\partial \sigma_{ij}}{\partial x_j} + \rho f_i \qquad (3)$$

where the entire stress tensor is denoted by the symbol $\boldsymbol{\sigma} = (\sigma_{ij})$, pressure is represented by the symbol p, velocity components are denoted by v_i, and body forces are denoted by f. Rheology provides an explanation for the relationship that exists between the total stress tensor and the other variables. The equation for the total stress tensor, σ, for the incompressible generalised Newtonian fluid may be written as follows:

$$\sigma_{ij} = -p\delta_{ij} + 2\mu d_{ij},$$

The rate of strain tensor,$\mathbb{D} = (d_{ij})$, can be written as follows:

$$d_{ij} = \frac{1}{2}\left(\frac{\partial v_i}{\partial x_j} + \frac{\partial v_j}{\partial x_i}\right) \qquad (4)$$

Furthermore, the viscosity coefficient, denoted by the symbol μ, is a function $\mu = \mu(\mathbb{D})$.

After that, the starting and boundary conditions that are appropriate for the system of equations (3) and (2) are determined.

The viscosity function, denoted by $\mu = \mu(\mathbb{D})$, is dependent on the rate of strain tensor $\mathbb{D}$, also known as the shear rate, denoted by e $\dot{\gamma} = \sqrt{2\sum_{ij} d_{ij}^2}$, as a result, the viscosity function may be interpreted as follows:

$$\mu = \mu(\dot{\gamma}). \qquad (5)$$

In the study, the Herscheley-Buckley fluid extension of the Bingham fluid is explored using the constitutive equation provided by $\tau = \tau_0 + \mu_0 \dot{\gamma}^{\alpha}$, that is More specifically, the viscosity is given by $\mu = \tau_0 \dot{\gamma}^{-1} + \mu_0 \dot{\gamma}^{\alpha-1}$, where the power coefficient $\alpha \geqslant 0$, μ_0 is the plastic viscosity, and, τ_0 is the yield stress. Newtonian fluid is recovered when $\tau_0 = 0$ and $\alpha = 1$, whereas Newtonian fluid is not recovered when r $\tau_0 = 0$ and,

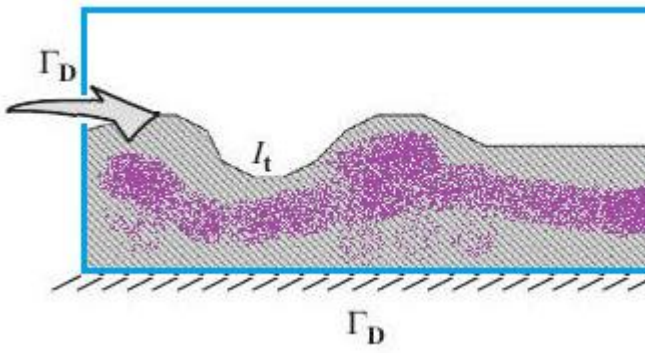

Figure 1: A representation of Unconfined surface flow as the flow of two fluids.

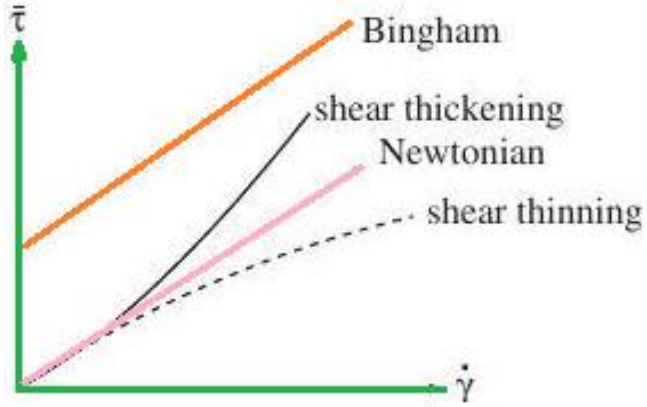

Figure 2: Depicts the relationship between the shear stress and the shear rate for Bingham fluids.

$\alpha \neq 1$ provides us with the power law fluid (shear-thinning fluids or fluids that thicken when subjected to shear). In each of these scenarios, the Bingham fluid was successfully reclaimed for the case $\tau_0 > 0$ and $\alpha = 0$. Figure 2 depicts the relationship between the shear stress, denoted by τ, and the shear rate, denoted by $\dot{\gamma}$.

In what follows, we will use the same notation for either the constant viscosity $\mu =$ constant. or the viscosity function $\mu = \mu(\dot{\gamma})$ of the generalised Newtonian fluid. Both of these notations will be explained in more detail below.

1.2. A FORMULATION WITH TWO PHASES

The model is defined with the assistance of two phases in order to be able to explain the Unconfined surface flow in complicated geometries, where the fluid motion might meet barriers that are far removed from the original configuration (let us distinguish the two phases as liquid and gas). The initial configuration with the fixed walls is filled with two different fluids: the first fluid, which is liquid, is the fluid that we are interested in, and the other fluid, which is gas, is the surrounding fluid that fills up the remaining room in the configuration (see Figure. 1 for an illustration of this). Considered here are the two fluids, each of which has a density of ρ_k, together with their velocities of $\mathbf{v}^{(k)}$, pressures of $p^{(k)}$, and viscosities of μ_k. The region of space that is occupied by the k th fluid at time t is indicated by the symbol $\Omega_t^{(k)}$, and the motion of the fluid is defined by the equation (3) when applied to the region of space denoted by on the domain $\Omega_t^{(k)}$ for $k = 1,2$ in conjunction with the continuity equation (2). (Figure. 1).

In addition to this, the kinematic requirement $\mathbf{v}^{(1)} = \mathbf{v}^{(2)}$ and the dynamic condition $\boldsymbol{\sigma}^{(1)} \cdot \mathbf{n} = \boldsymbol{\sigma}^{(2)} \cdot \mathbf{n}$ are both required on the interface $\mathcal{I}_t$ (There is no presumption of surface tension.).

In accordance with (S.R. Ransau, 2002), we are able to introduce the functions ρ, μ and $\mathbf{v}$, which are defined on the computational domai n $\Omega = \Omega_t^{(1)} \cup \Omega_t^{(2)}$ as $\rho = \rho_k, \mu = \mu_k$ and $\mathbf{v} = \mathbf{v}^{(k)}$ on the domain $\Omega_t^{(k)}$ for $k = 1,2$. If this is the case, the issue may be formulated as follows on the domain Ω:

$$\rho \frac{\partial v_i}{\partial t} + \rho \sum_j \frac{\partial (v_i v_j)}{\partial x_j} + \frac{\partial p}{\partial x_i} = \sum_j \frac{\partial (\mu d_{ij})}{\partial x_j} + \rho f_i,\ \rho \nabla \cdot \mathbf{v} = 0 \quad (6)$$

1.3. LEVEL SET METHOD

Problems may arise in Unconfined surface modelling as a result of either the mathematical modelling (such as the moving interface or the physical transfer process across the surface), or the numerical approximation (e.g., approximation of the moving interface, discontinuity of physical quantities-density, viscosity, pressure-across the interface). The techniques of Unconfined surface approximation may be separated into two categories: those that include interface tracking (in which the interface is approximated in its entirety) and those that involve interface capturing (in which the interface is captured entirely) (the fluid volume is tracked rather than interface). The level set approach is used in this piece of research (for examples, see: (J.A. Sethian, 1999). Equation (6) is connected to the transfer equation for the level set function, which is denoted by φ.

$$\frac{\partial \varphi}{\partial t} + \nabla \cdot (\mathbf{v}\varphi) = 0 \qquad (7)$$

where the meaning of the function φ at a position $\mathbf{x}$ shows whether it is inhabited by the fluid ($\varphi > 0$) or by the gas ($\varphi < 0$), depending on whether or not it is above or below the zero line. On the surface $\varphi = 0$ holds is true.

The Weber number, which can be calculated using the formula $e = \rho U^2 L/\eta, \eta$, where is the coefficient of surface tension, must be of order one or less for the surface tension to be significant. In this particular scenario, the Weber number is assumed to be $We \gg 1$, and the surface tension is left out of the equation.

With the use of the Heavyside function, the parameters of density, viscosity, and velocity may be determined.

$$\rho = \rho_1 + H(\varphi)(\rho_2 - \rho_1) \text{ and } \mu = \mu_1 + H(\varphi)(\mu_2 - \mu_1) \qquad (8)$$

where the Heavyside $H(\varphi) = 1$ when $\varphi > 0, H(\varphi) = 0$ when $\varphi < 0$ and $H(0) = \frac{1}{2}$. In the numerical simulations, the regularised Heavyside function s H_ε are used, and the parameter is used to control the thickness of the interface. This allows the thickness of the interface to be customized ε.

2. DISCRETIZATION

2.1. TIME DISCRETIZATION

First, let's talk about how the issue is discretized over different time periods. We take into account a partition of the time range $0 = t_0 < t_1 < \cdots < T, t_k = k\Delta t$, with a time step $\Delta t > 0$ that is greater than 0, and we use vn as an approximation for the solution $\mathbf{v}(t_n)$ (that is specified as Ω_{t_n}) at time t_n by $\mathbf{v}^n$. We employ a second-order two-step technique for the time discretization, using the calculated approximate solution $\mathbf{v}^{n-1}$ and $\mathbf{v}^n$ in Ω in for the computation of $\mathbf{v}^{n+1}$. For further information, see "Time Discretization." Then, on each time level t_{n+1},, the issue of identifying unknown functions $\mathbf{v}^{n+1}: \Omega \to \mathbb{R}^2$ and $p^{n+1}, \mu^{n+1}, \rho^{n+1}: \Omega \to \mathbb{R}$ that fulfil the equations is presented as a result of the second-order, two-step time discretization.

$$\rho^{n+1}\frac{3\mathbf{v}^{n+1} - 4\mathbf{v}^n + \mathbf{v}^{n-1}}{2\Delta t} + \rho^{n+1}(\mathbf{v}^{n+1} \cdot \nabla)\mathbf{v}^{n+1} + \nabla p^{n+1} = \nabla \cdot (\mu^{n+1}\mathbb{D}) + \rho^{n+1} f_i$$
$$\rho^{n+1}\text{div } \mathbf{v}^{n+1} = 0$$

inside the computing area Ω, with the Dirichlet border requirements being met. [Note:] Also discretized in time is the transport equation for the level set function (7).

$$\frac{3\varphi^{n+1} - 4\varphi^n + \varphi^{n-1}}{\Delta t} + \nabla \cdot (\mathbf{v}^{n+1}\varphi^{n+1}) = 0 \qquad (10)$$

in addition to ρ^{n+1} along with μ^{n+1} are then specified by equation. (8).

2.2. Spatial discretization

The so-called weak formulation serves as the point of departure for the finite element discretization of issue (9). In order to do this, we will use the simplified notatio n $\rho := \rho^{n+1}, \mathbf{v} := \mathbf{v}^{n+1}, p := p^{n+1}, \mu := \mu^{n+1}$ and we will write system (9) in the following format:

$$\rho\frac{3\mathbf{v} - 4\mathbf{v}^n + \mathbf{v}^{n-1}}{2\Delta t} + \rho(\mathbf{v} \cdot \nabla)\mathbf{v} + \nabla p = \nabla \cdot (\mu\mathbb{D}) + \rho f_i,$$
$$\rho\text{div } \mathbf{v} = 0 \qquad (11)$$

The velocity spaces W and X, as well as the pressure space, are defined as follows:

$$W = (H^1(\Omega))^2,\ X = \{\mathbf{N} \in W; \mathbf{N}|_{\Gamma_D} = 0\},\ Q = L^2(\Omega),$$

transform the terms containing $\nabla \cdot (\mu\mathbb{D})$ and ∇p with the aid of Green's theorem, we find that the solution $U = (\mathbf{v}, p)$ of the problem of Eqs. (10) satisfies the condition $a(U, U, V) = f(V)$ for all $V = (\mathbf{N}, q) \in X \times Q$. The forms are defined

where $L^2(\Omega)$ is the space of square integrable functions in the Lebesgue transform over the domain (Ω) and $H^1(\Omega)$ represents the Sobolev space that contains square integrable functions and the first-order derivatives of those functions. Over the domain, both of these spaces are defined to exist. If we now multiply the first and second equations in the product (10) by any function, we get the following:

$$\mathbf{N} \in X \text{ and } q \in Q,$$

respectively, add them up, integrate over Ω, and use Green's theorem to transform the terms containing $\nabla \cdot (\mu\mathbb{D})$ and ∇p, we will discover that the solutio n

$U = (\mathbf{v}, p)$ of the problem posed by equation (10) persuades the condition $a(U, U, V) = f(V)$ for all $V = (\mathbf{N}, q) \in X \times Q$. There is a definition of the forms.

$$a(U^*, U, V) = \frac{3}{2\Delta t}(\rho\mathbf{v}, \mathbf{N})_\Omega + (\mu\nabla\mathbf{v}, \nabla\mathbf{N})_\Omega + (\rho(\mathbf{v}^* \cdot \nabla)\mathbf{v}, \mathbf{N})_\Omega - (p, \nabla \cdot \mathbf{N})_\Omega + (\nabla \cdot \mathbf{v}, q)_\Omega,$$
$$f(V) = \left(\rho\frac{4\mathbf{v}^n - \mathbf{v}^{n-1}}{2\Delta t} + \rho f_i, \mathbf{N}\right)_\Omega$$

(11)

$U = (\mathbf{v}, p)$, $V = (\mathbf{N}, q), U^* = (\mathbf{v}^*, p)$. In order to use the Galerkin finite element method, we first make approximations of the spaces W, X, and Q based on the weak formulation using subspaces of finite dimensions. $W_\Delta, X_\Delta, Q_\Delta, \Delta \in (0, \Delta_0), \Delta_0 > 0, X_\Delta = \{\mathbf{v}_\Delta \in W_\Delta; \mathbf{v}_\Delta|_{\Gamma_D} \cap \Gamma_{Wt} = 0\}$. Therefore, in order to get an approximate solution, we will define the discrete issue. $U_\Delta = (\mathbf{v}_\Delta, p_\Delta) \in W_\Delta \times Q_\Delta$ such that $\mathbf{v}_\Delta$ roughly meets the Dirichlet boundary criteria, as well as the identity condition

$$a(U_\Delta, U_\Delta, V_\Delta) = f(V_\Delta) \text{ for all } V_\Delta = (\mathbf{v}_\Delta, q_\Delta) \in X_\Delta \times Q_\Delta$$
(12)

It is necessary for the Babuka-Brezzi (BB) condition to be met by the pair of finite element spaces denoted by (X_Δ, Q_Δ). However, this issue may be remedied with the use of Galerkin Least Squares stabilisation (see to cf. for more reading) (T.J.R. Hughes, et. al., 1989).

Assuming that the domain Ω is a polygonal approximation of the area inhabited by the fluid at tim e t_{n+1}, we do practical calculations under the assumption that the space s $W_\Delta, X_\Delta, Q_\Delta$ are defined over a triangulation $\mathcal{T}_\Delta$ of the domain Ω, which is created by a limited number of closed triangle s $K \in \mathcal{T}_\Delta$. At this point Δ the size of the mesh is denoted by the letter $\mathcal{T}_\Delta$ here. Piecewise polynomial functions are responsible for the formation of the spaces $_\Delta, X_\Delta$ and, Q_Δ. For the purpose of our calculations, the equal order choice of piecewise linear finite P_1/P_1 nonconforming components has been used for the purpose of approximating the velocity and pressure.

2.3. STABILIZATION OF THE FEM

When applied to problems with large Reynolds numbers, the conventional Galerkin discretization (12) may generate approximations of solutions that are plagued by spurious oscillations. The Galerkin Least Squares approach is employed for the purpose of stabilising in order to circumvent this disadvantage. The following terms constitute the stability criteria;

$$\mathcal{L}_\Delta(U^*, U, V) = \sum_{K\in\mathcal{T}_\Delta} \delta_K\left(\frac{3}{2\Delta t}\rho\mathbf{v} - \nabla \cdot (\mu\mathbb{D}) + \rho(\mathbf{v}^* \cdot \nabla)\mathbf{v} + \nabla p\right.$$
$$\mathcal{F}_\Delta(V) = \sum_{K\in\mathcal{T}_\Delta} \delta_K\left(\frac{\rho}{2\Delta t}(4\mathbf{v}^n - \mathbf{v}^{n-1}) + \rho f_i, \psi(V)\right)_K$$

where $U = (\mathbf{v}, p)$, $V = (\mathbf{N}, q), U^* = (\mathbf{v}^*, p), \psi(V) = \rho(\mathbf{v}^* \cdot \nabla)\mathbf{N} + \nabla q, (\cdot,\cdot)_K$ signifies the scalar product in $L^2(K)$, and $\delta_K \geqslant 0$ are parameters that have been set in an appropriate manner. In addition, the added grade-level and divisional stabilising

$$\mathcal{P}_\Delta(U, V) = \sum_{K\in\mathcal{T}_\Delta} \tau_K(\rho\nabla \cdot \mathbf{v}, \nabla \cdot \mathbf{N})_K$$

is introduced with suitably chosen parameters $\tau_K \geqslant 0$.

The stabilized discrete problem reads: find $U_\Delta = (\mathbf{v}_\Delta, p_\Delta) \in W_\Delta \times Q_\Delta$ such that $\mathbf{v}_\Delta$ satisfies approximately Dirichlet boundary conditions and

is presented with parameters $\tau_K \geqslant 0$ that have been selected appropriately.

The statement for the stabilised discrete issue is as follows:

Discover $U_\Delta = (\mathbf{v}_\Delta, p_\Delta) \in W_\Delta \times Q_\Delta$ such that $\mathbf{v}_\Delta$ fulfils roughly Dirichlet boundary conditions and p_Δ satisfies approximately Dirichlet boundary conditions.

$$a(U_\Delta, U_\Delta, V_\Delta) + \mathcal{L}_\Delta(U_\Delta, U_\Delta, V_\Delta) + \mathcal{P}_\Delta(U_\Delta, V_\Delta) = f(V_\Delta) + \mathcal{F}_\Delta(V_\Delta)$$

(13)

in spite of $V_\Delta = (N_\Delta, q_\Delta) \in X_\Delta \times Q_\Delta$.

The parameters δ_K and $\tau_K$are selected in accordance with (T. Gelhard, 2005) by taking into account the

local transport velocity $\mathbf{v}^*$, the local mesh size h, and the local viscosity μ, to be more specific:

$$\delta_K = \left(\frac{4\mu}{h^2} + 2\|\rho v^*\|_K + \frac{\|\rho\|_K}{\tau}\right)^{-1},\ \tau_K = \frac{h^2}{\delta_K} \quad (14)$$

2.4. LEVEL SET FUNCTION NUMERICAL APPROXIMATION

The numerical approximation of the transport equation (7) may be accomplished using the finite element approach or the finite volume method, respectively cf (R.J. LeVeque, 1990). Both of these approaches were put to the test by the algorithm that was explained. To begin, when the finite volume technique is used, the function φ is approximated by the piecewise constant function on every element φ_Δ, which may be written as $K \in \mathcal{T}_\Delta$, i.e., $\varphi_\Delta = \varphi_K$ on $K \in \mathcal{T}_\Delta$. In other words, is equal to on $K \in \mathcal{T}_\Delta$. Then, by using Equation (7), integrating over an element K, moreover applying Green's Theorem, we are able to get

$$\frac{\mathrm{d}\varphi_K}{\mathrm{d}t} = \frac{1}{|K|}\sum_{S\in\partial K}\int_S \varphi_S(\mathbf{v}\cdot\mathbf{n})\mathrm{d}S \quad (15)$$

where $S \in \partial K$ designates all boundary sides of the element K, φ_Kdenotes the constant value of the function φ on the element K, where φ_S represents all boundary sides S of the element K. It is possible to calculate the function value dS on the side S by either using the upwind approach or with the assistance of Lax-Friedrichs method; for an example of the latter, see R.J. LeVeque's book (1990). It is necessary to discretize the time derivative $(\mathrm{d}/\mathrm{d}t)\varphi_K$. For example, the explicit Euler technique may be achieved by using the forward difference formula $\mathrm{d}\varphi_K/\mathrm{d}t \approx (\varphi_K^{n+1} - \varphi_K^n)/\Delta t$. Increasing the order of time discretization may be accomplished by the use of the higher-order time difference formula (also known as the three-step formula or the Runge-Kutta procedures). It is possible to enhance the order of the space discretization by using techniques such as piecewise linear reconstruction, for instance.

The discretization of the issue might also be done with the help of the finite element technique. This is the alternative option. The test function ψ is multiplied by the equation (7), and the result is integrated across the domain Ω. The Dirichlet boundary conditions for are specified on the inlet portion of the boundary represented by the notation $\Gamma_- = \{\mathbf{x} \in \partial\Omega: \mathbf{v}\cdot\mathbf{n} < 0\}$. After that, the unstable formulation is made stable by using the very consistent approach.

$$\int_\Omega \frac{\partial\varphi}{\partial t}\psi\mathrm{d}x + \int_\Omega \nabla\cdot(\mathbf{v}\varphi)\psi\mathrm{d}x + \sum_K \delta_1 \frac{h}{\|\mathbf{v}\|_K}\left(\frac{\partial\varphi}{\partial t} + \nabla\cdot(\mathbf{v}\varphi), \mathbf{v}\cdot\nabla\psi\right)_K = 0 \quad (16)$$

While it is assumed here for the sake of simplicity that $\|\mathbf{v}\|_K > 0$ is greater than 0 on every element K, cf (A. Quarteroni, A. Valli, 1994). The time derivative, denoted by $\partial\varphi/\partial t$, may be estimated with the help of the formula for the time difference obtained by doing three steps:

$$\frac{\partial\varphi}{\partial t} \approx \frac{3\varphi^{n+1} - 4\varphi^{n+1} + \varphi^{n+1}}{\Delta t}$$

It is necessary for the level set algorithm to include a reinitialization phase in order to guarantee that the level set function will continue to behave as a distance function φ throughout the calculation (M. Sussman, et. al., 1998). In this instance, the alternative methodology that involves algebraically reconstructing the function φ is used. In this instance, the method shown below is used:

- set $\tilde{\varphi}_\Delta(x_i) = +\infty$ for all vertices x_i of the triangulation $\mathcal{T}_\Delta$,
- for all triangles $K \in \mathcal{T}_\Delta$ with vertices A, B, C,
- condition $\varphi(A)\varphi(B)\varphi(C) < 0$ then

a) locate the point of intersection. $\mathcal{M} = K \cap \mathcal{I}_{\Delta,t}$ (line/vertex),

b) Calculate the distance d from the centre point $\mathcal{M}$ to each of the vertices x_i of the triangle $\mathcal{T}_\Delta$ (for interface neighbouring

vertices the mass conservation principle must be satisfied),

c) set $\tilde{\varphi}_\Delta(x_i) = \min(\tilde{\varphi}_\Delta(x_i), d)$,

d) for all vertices x_i set $\varphi_\Delta(x_i) := \tilde{\varphi}_\Delta(x_i)\text{sgn}\ \varphi_\Delta(x_i)$.

2.5. NONLINEAR PROBLEM SOLUTION AND CONNECTION

Solve the linearized problem (13) performed and new approximation of the velocity **v** is obtained.

After then, the following procedure is used to each time step t_n in order to solve the nonlinear issue (16) in conjunction with the previous one (13), which reads as follows:

(1) By extrapolating the estimates of the previous time steps $(\mathbf{v}_\Delta^n, \mathbf{v}_\Delta^{n-1})$, we may get an approximation of the velocity at the next time level $t^{n+1}, \mathbf{v}_\Delta \approx \mathbf{v}(t_{n+1})$..
(2) You may get the approximation function $\varphi_\Delta$by using the velocity $\mathbf{v}_\Delta$ and solving equation (13).
(3) Calculate the rate of shear as well as the components d_{ij} of the strain tensor $\mathbb{D}$ for each and every element $K \in \mathcal{T}$
(4) Determine the liquid/gas viscosity by using the formula $\mu = \mu_k(\dot{\gamma})$ on each and every element $K \in \mathcal{T}_\Delta$.
(5) Make the necessary adjustments to $\rho \approx \rho(t_{n+1})$ in addition to $\mu = \mu(t_{n+1})$ by using the equation (8).
(6) After performing the steps necessary to solve the linearized problem (13), a new estimate of the velocity **v** was achieved.
(7) Carry on with step (b) until convergence has been reached.
(8) Set $\mathbf{v}^{n+1} := \mathbf{v}, p^{n+1} := p, \rho^{n+1} := \rho$ and $\mu^{n+1} := \mu, n := n+1$ and proceed on the next time level.

In order to find a solution to the issue (13), which pertains to the constitutive equation (5), more treatment is required. When there is no longer any shear strain rate magnitude, the Bingham constitutive model is no longer able to predict the shear stresses. Several writers have suggested that the Bingham constitutive equation be modified in such a way that the solid regime $(\tau < \tau_0)$ is replaced with an extremely viscous regime. For reference, see the following: (E. Mitsoulis, T. Zisis, 2001). After making this adjustment, the series of linearized problems is used to accomplish the solution to the issue (13). After that, the linearized issue is solved with the assistance of the UMFPACK direct solver, is a collection of programmes that use the Unsymmetric MultiFrontal approach to solve unsymmetric sparse linear problems of the form Ax=b (Matrix A is not required to be symmetric). which may be referenced here.

3. Numerical results and conclusions

The approach was evaluated using a variety of different scenarios. To begin, a computation was made to determine the flow of a Bingham fluid in a lid-driven cavity flow (see also cf). (D. Vola, et. al., 2003) Figure 3 displays the findings of the numerical analysis.

In conclusion, the numerical solution to the standing wave issue is shown in figure 4, which pertains to the Newtonian fluids scenario (air and water). The initial interface between the liquid and gas phases was established by the equation $10y - x = 6$, and the vertical gravity force with the acceleration $g = 10\ \text{m s}^{-2}$ was applied to it. The liquid and gas phases were then separated by the interface. Figure 4 provides a visual representation of the Unconfined surface oscillations.

In this work, the modified GLS approach is extended to the issue of Unconfined surface, and the study presents that extension. The fluids that are being taken into consideration are generic Newtonian fluids. The approach was put to the test for a variety of issues, and the outcomes of the non-Newtonian fluid flow in the lid-driven cavity as well as the standing wave difficulties for the Newtonian fluid case are displayed.

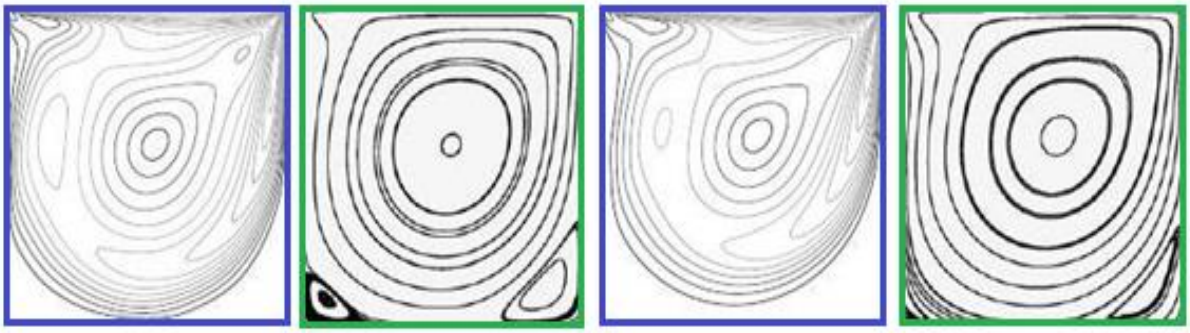

Figure 3: A graphical representation of a numerical simulation of a Newtonian and Bingham fluid in a lid-driven hollow. a Newtonian fluid with a viscosity of $\mu = 10^{-3}$ and a Bingham fluid with characteristics of $\tau_0 = \frac{1}{\sqrt{2}}10^{-3}$, respectively. Streamlines that have stiff zones and isolines that measure the magnitude of the velocity.

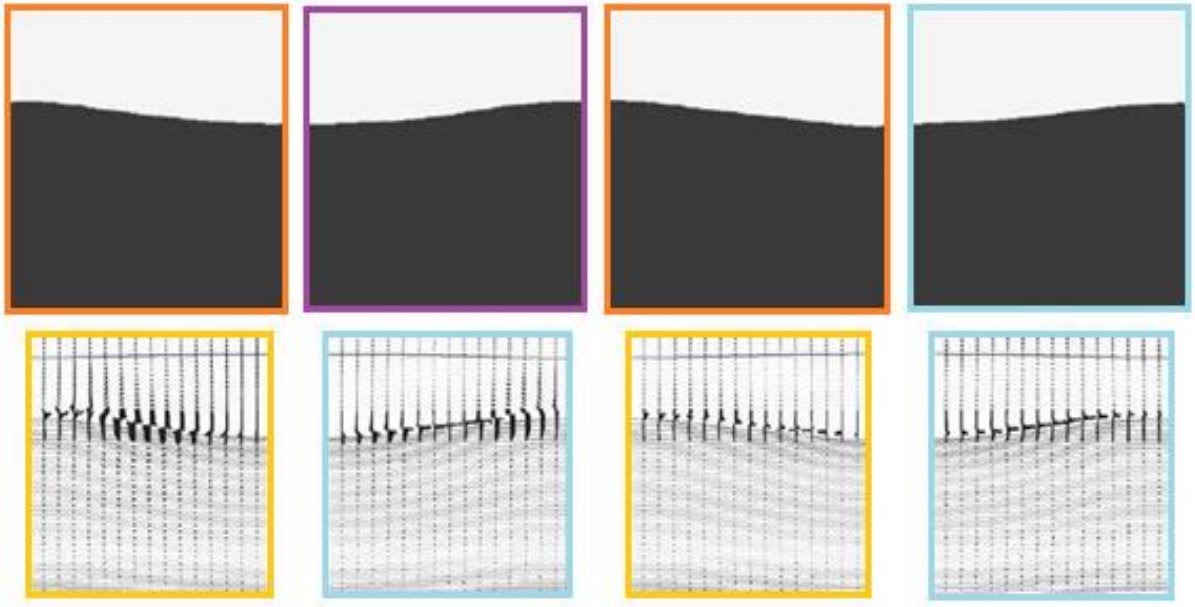

Figure 4: The standing wave benchmark was modelled using numerical simulation. The density, denoted by ρ, is shown in the top row, while the pressure field and velocity vectors are shown in the row below it.

REFERENCES

[1] Quarteroni, A. Valli, Numerical Approximation of Partial Differential Equations, Springer, Berlin, 1994.

[2] Patzák, Z. Bittnar, Simulation of fresh concrete flow, in: Proceedings of the Fifth International Conference on Engineering Computational Technology [CD-ROM], Stirling: Civil-Comp Press Ltd., 2006, ISBN 1-905088-11-6.

[3] Ferraris, F. de Larrard, N. Martys, Fresh concrete rheology: recent developments, in: S. Mindess, J. Skalny (Eds.), Materials Science of Concrete IV, The American Ceramic Society, 2001, pp. 215-241.

[4] Beaupre, S. Mindess, Rheology of fresh concrete: principles, measurement and applications, in: S. Mindess, J. Skalny (Eds.), Materials Science of Concrete V, The American Ceramic Society, 1998, pp. 149-180.

[5] Vola, L. Boscardin, J.C. Latche, Laminar unsteady flows of Bingham fluids: a numerical strategy and some benchmark results, J. Comput. Phys. 187 (2003) 441–456.

[6] J.A. Sethian, Level Set Methods and Fast Marching Methods, second ed., Cambridge Monograph on Applied and Computational Mathematics, Cambridge University Press, Cambridge, UK, 1999.

[7] M. Sussman, E. Fatemi, P. Smereka, S. Osher, An improved level set method for incompressible two-phase flows, Comput. & Fluids 27 (1998) 663-680.

[8] P. Coussot, S. Proust, C. Ancey, Viscoelastic interpretation of deposits of yield stress fluids, J. Non-Newtonian Fluid Mech. 66 (1996) 55-70.

[9] R. Codina, Stabilization of incompressibility and convection through orthogonal sub-scales in finite element methods, Comput. Method Appl. Mech. Eng. 190 (2000) 1579-1599.

[10] R.B. Bird, R.C. Armstrong, O. Hassager, Dynamics of Polymeric Liquids, vol. 1, Fluid Mechanics, Wiley, New York, 1987.

[11] R.J. LeVeque, Numerical Methods for Conservation Laws: Lectures in Mathematics, Birkhauser, Basel, 1990.

[12] R.P. Chhabra, J.F. Richardson, Non-Newtonian Flow in the Process Industries, Butterworth-Heinemann, London, 1999.

[13] S.R. Ransau, Solution methods for incompressible viscous Unconfined surface flows: a literature review, Technical Report 3/2002, Norwegian University of Science and Technology, Trondheim, 2002.

[14] T. Gelhard, G. Lube, M.A. Olshanskii, J.-H. Starcke, Stabilized finite element schemes with LBB-stable elements for incompressible flows, J. Comput. Appl. Math. 177 (2005) 243-267.

[15] T.J.R. Hughes, L.P. Franca, G.M. Hulbert, A new finite element formulation for computational fluid dynamics: VIII. The Galerkin/least-squares method for advective-diffusive equations, Comput. Methods Appl. Mech. Eng. 73 (1989) 173-189.